Published in final edited form as:
Biochem Biophys Res Commun. 2013 October 18; 440(2): . doi:10.1016/j.bbrc.2013.08.055.

A Humanin Analog Decreases Oxidative Stress and Preserves Mitochondrial Integrity in Cardiac Myoblasts

Laura E. Klein, **Lingguang Cui**, **Zhenwei Gong**, **Kai Su**, and **Radhika Muzumdar**
Department of Pediatrics, Albert Einstein College of Medicine, Bronx, NY 10461

Abstract

A potent analog (HNG) of the endogenous peptide humanin protects against myocardial ischemia-reperfusion (MI-R) injury *in vivo*decreasing infarct size and improving cardiac function. Since oxidative stress contributes to the damage from MI-R we tested the hypotheses that: 1. HNG offers cardioprotection through activation of antioxidant defense mechanisms leading to preservation of mitochondrial structure and that, 2. the activity of either of a pair of non-receptor tyrosine kinases, c-Abl and Arg is required for this protection. Rat cardiac myoblasts (H_9C_2 cells) were exposed to nanomolar concentrations of HNG and to hydrogen peroxide (H_2O_2). Cells treated with HNG in the presence of H_2O_2 demonstrated reduced intracellular reactive oxygen species (ROS), preserved mitochondrial membrane potential, ATP levels and mitochondrial structure. HNG induced activation of catalase and glutathione peroxidase (GPx) within 5 minutes and decreased the ratio of oxidized to reduced glutathione within 30 minutes. siRNA knockdown of both Abl and Arg, but neither alone, abolished the HNG-mediated reduction of ROS in myoblasts exposed to H_2O_2. These findings demonstrate an HNG-mediated, Abl- and Arg-dependent, rapid and sustained activation of critical cellular defense systems and attenuation of oxidative stress, providing mechanistic insights into the observed HNG-mediated cardioprotection *in vivo*.

Keywords

humanin; mitochondria; myocardial ischemia-reperfusion; oxidative stress

1. INTRODUCTION

Coronary heart disease is the major cause of heart disease resulting in about 1 out of every 5 deaths [1]. Besides immediate risks, around 20% of those experiencing myocardial infarct will also develop heart failure [2]. Though reperfusion is critical for cardiac myocyte survival, minimizing the ventricular wall stress that favors remodeling, enlargement and heart failure [3], most cell death and long-term damage to cardiac function also occur at this stage.

Influx of oxygen and recovery of mitochondrial respiration during the reperfusion phase increase reactive oxygen species (ROS), levels of which are known to increase following

Corresponding author: Radhika Muzumdar, Department of Pediatrics, Albert Einstein College of Medicine, 1300 Morris Park Avenue, Golding 705, Bronx, NY, USA, 10461, Tel.: (718) 430-3295; Fax: (718) 654-4161, radhika.muzumdar@einstein.yu.edu.

many pathologic situations including MI-R [4, 5, 6]. Calcium uptake into the mitochondria via the calcium uniporter and loss of mitochondrial membrane potential (MMP) were recently shown to occur during reperfusion [7]. Increased ROS overwhelms normal antioxidant defenses and favors the opening of the mitochondrial permeability transition pore, leading to further membrane depolarization, ATP hydrolysis and mitochondrial swelling leading to rupture of the outer membrane and release of pro-death proteins into the cytosol [8]. Since ROS are important eukaryote cell signals, the generation of hydrogen peroxide is tightly regulated as are localization, expression and activation of antioxidant enzymes [9, 10]. Major players in cell defense against excessive ROS include non-enzymatic small molecule antioxidants such as glutathione and enzymes that include superoxide dismutase (SOD), catalase and glutathione peroxidase (GPx).

Our lab has been investigating a highly potent analog of the endogenous, 24-aa peptide Humanin (HN), HNG (HN in which the serine 14 is replaced by glycine). Originally isolated from a protected lobe of a brain from an Alzheimer's disease patient, HN has been shown to be neuroprotective and also protects other cell types from a variety of insults. A role for HN in cardiovascular diseases has been shown by us and others [11, 12, 13, 14, 15]. Circulating humanin levels in humans were recently found to be associated with impaired microvascular coronary endothelial function [16]. HN is highly expressed in unstable carotid plaques in atherosclerotic patients, with higher levels found in symptomatic patients relative to the asymptomatic group [17]. We previously showed that HNG administration protected against MI-R injury in a mouse model, decreasing infarct size and improving LV function [18].

The translational promise shown by HN in cardiovascular disorders underscores the need for a more mechanistic understanding of its action in the heart. The involvement of oxidative stress in the injury produced by MI-R led us to hypothesize that the mechanism of the cardioprotection provided by HNG may involve mitigation of oxidative stress and activation of antioxidant defense mechanisms.

2. MATERIALS AND METHODS

2.1. Cell culture

Low passage (< 15) H_9C_2 cells (ATCC, CRL-1446) were grown at 37°C in 10% CO_2 in DMEM with D-glucose (1000 mg/L), L-glutamine (584 mg/L), sodium pyruvate (1 mM) and 10% FBS (Biowest). For ROS determination and JC-10 staining, the same growth medium was used without phenol red.

2.2. ROS determination

H_9C_2 cells were grown to 70% confluence in black, 96-well plates. Four of the eight wells in each column were loaded with a 10μM solution of a thiol reactive, non-fluorescent chloromethyl derivative of DCF (Molecular Probes, C6827), the other four with only PBS as controls for auto-fluorescence. After loading, the plate was reacted for 40 minutes at 37°C in growth medium containing control (saline) or HNG with or without H_2O_2 (100μM). Fluorescence measurements were obtained at 485 excitation/535 emission using a Molecular Devices SpectraMax M5e scanning spectrophotometer.

2.3. Measurement of Mitochondrial transmembrane potential (Δψm)

HNG effects on MMP changes were assessed using the fluorochrome dye JC-10 (Enzo Life Sciences). H_9C_2 cells seeded in black, 96-well, at 70% confluence were treated with growth media containing either the saline or HNG (10nM) and H_2O_2 (40 μM) for 30 minutes at 37°C. This media was aspirated and replaced with 1X Hanks buffered salt solution containing 20 mM Hepes and 20μM JC-10 and the plate was incubated for an additional 30

minutes at 37°C. After 3 rinses with wash buffer (1X HBSS, 10 mM Hepes and 0.02mg/100ml D-glucose), the fluorescent signal was read on a Molecular Devices SpectraMax M5e scanning spectrophotometer using 490 and 525 nm as green excitation and emission wavelengths, respectively (cutoff 515 nm) and 490 and 590 nm as red excitation and emission wavelengths, respectively (cutoff 570 nm). The ratio of the reading at 590 nm to that at 525 nm was considered as the relative $\Delta\psi m$ value.

2.4. Assessment of mitochondrial function via determination of intracellular ATP

H_9C_2 cells were treated for the indicated time with saline or HNG (10 nM). ATP was extracted as previously described [19]. Briefly, cells were dispersed into 85 mM sodium citrate, extracted with a final concentration of 2.3% TCA, neutralized with Tris-acetate EDTA buffer (0.1M Tris, pH 7.75 with acetic acid, 2mM EDTA) and boiled for 3 minutes. ATP levels were measured with a Bioluminescent Assay Kit (Sigma-Aldrich, St. Louis, MO, USA, FL-AA) and readings taken by a BMG LABTECH FLUOstar OPTIMA multimode microplate reader (Ortenberg, Germany).

2.5. Immunofluorescence

H_9C_2 cells growing on polylysine-coated coverslips were pretreated for 10 minutes with saline or HNG and then exposed to 100 μM H_2O_2 for 3 hours in the presence or absence of HNG. Cells were loaded with Mitotracker Red CMXROS (Molecular Probes, M-7512), fixed with 3% formaldehyde and 0.02% glutaraldehyde for 30 minutes at room temperature, permeablized with 0.1% Triton X-100 for 5 minutes and labeled with anticytochrome-c followed by an Alexa Fluor-488, green fluorescent secondary antibody (Jackson ImmunoReach Laboratories, Inc.) and dapi prior to fluorescence photography. Photographs were prepared with a Zeiss Axioskop II microscope with Zeiss Axiovision software and fitted with fluorescence filters for dapi, FITC and Rhodamine, at 63× magnification.

2.6. Assays for non-enzymatic and enzymatic antioxidant activity

The level of the oxidized disulfide dimer (GSSG) and the reduced form of glutathione (GSH) was determined in lysates from H_9C_2 cells treated for various time points with HNG (10 nM). These values were obtained by carrying out a series of reactions as described by the Glutathione assay kit (Cayman Chemical Company, catalog # 703002). Assays for determination of enzyme activities—total superoxide dismutase (SOD), catalase and glutathione peroxidase (GPx) (BioVision Research Products, catalog #s K335, K773 and K762, respectively) were performed, as instructed, on H_9C_2 cell lysates following treatment with either saline or HNG (10nM) at the time points indicated. These values were normalized to total protein in the lysates.

2.7. Abl and Arg knockdowns

Synthetic siRNAs for Abl and for control transfections were obtained from Qiagen. The sequence used to knockdown Abl (RN_Abl1_4) was catalog number SI01484308. The siRNA sequence used to knockdown Arg was synthesized and purified by Integrated DNA Technologies, Inc. and the sequence was as follows: sense: 5’GGAAAUCAAGCAUCCUAAUUUAG3’, antisense: 5”UACUAAAUUAGGAUGCUUGAUUUCCUU3’. BLASTn searches were carried out to detect possible off targets for both siRNAs. AllStars_3 (catalog number SI04939025) siRNA was used as the positive control and AllStars Negative Control siRNA (catalog number 1027280) as the negative control in this optimization procedure. Transfections with siRNAs were performed in 6-well plates with 1.25×10^5 cells per well in 2.3 ml of growth medium for 72h before analyzing the degree of target knockdown. For immunoblots and Abl/Arg

knockdowns prior to seeding in 96-well black plates for ROS determinations, these conditions were scaled up to 100 mm dishes as described in the HiPerFect directions.

2.8. qRT-PCR

Total RNA was extracted from H_9C_2 cell cultures using RNAseasy Mini Kits μg of total RNA was reverse transcribed into cDNA using the Superscript III First-Strand Sysnthesis System (Invitrogen). The cDNA was then subjected to real-time PCR amplification using Light Cycler 480 SYBR Green I Master kit in a LightCycler® 480 Real –Time PCR System (Roche). The forward and reverse primers for each gene were as follows: Abl-cttgcaggaaaaccacctct and tctgggacagtttgtgagca; Arg-aaggcaaggagaggaatggt and ctggcactttgtggttgtg. The data were then normalized to the housekeeping gene RPL19-gaagaggaagggtactgccaac and tttttgaacacattccctttga.

2.9. Immunoblots

Cell lysates were prepared in RIPA buffer, resolved on SDS-PAGE gradient gels, transferred to PVDF membranes and probed with relevant antibodies (Abl: Abcam Inc, #10528, Arg: Epitomics, #5431-1, β-actin: Cell Signaling, #4967). Signals for Abl and Arg were normalized to the signal for the loading control, β-actin.

2.10. Statistics

All values result from a minimum of 3 experiments and are presented as means ± se. When appropriate, data were evaluated by the 2-sample Student's *t* test. A value of $p < 0.05$ was considered significant. To take into consideration false-positive associations resulting from multiple comparisons, the stringent Bonferroni correction was used; the value of *p* for inclusion was set to 0.05/5 = 0.01.

3. RESULTS

3.1. HNG maintains low intracellular ROS levels

Chloromethyl-DCF-loaded cells challenged with H_2O_2 showed an 86% increase in intracellular ROS compared with controls (1.7228 ± 0.1469 vs.0.9287± 0.1113). There was a 48% decrease in ROS, in HNG-treated cells relative to controls when both were challenged with 100 μM H_2O_2 (0.8998 ± 0.1650 vs.1.7228 ± 0.1469) (Fig. 1A). Levels of cellular ROS with HNG are comparable to the baseline (0.9287 ± 0.1113) and following treatment with ROS scavenger N-acetyl cysteine (NAC)(0.6687 ± 0.2090).

3.2. HNG preserves mitochondrial membrane potential (Δψm)

HNG produced a significant 11% increase in baseline Δψm (0.5226 ± 0.009 vs 0.5817 ± 0.007) (Fig. 1B). H_2O_2 (40 μM) decreased the membrane potential by 6% relative to the vehicle control alone (0.4901 ± 0.006 vs 0.5226 ± 0.009). In the presence of HNG (10 nM), the H_2O_2-induced decrease in the MMP was significantly attenuated, remaining at levels seen in the control group in the absence of H_2O_2 (0.5226 ± 0.009 vs 0.5128 ± 0.014).

3.3. HNG increases ATP production

There was a 92% increase in ATP levels at 30 minutes (95.41 ± 7.52 vs. 182.81 ± 18.60 pM/cell) and a 134% increase in 120 minutes (70.85 ± 5.58 vs. 165.89 ± 25.75 pM/cell) (Fig. 1C) in cells treated with HNG.

3.4. HNG preserves mitochondrial structural integrity

Immunofluorescence was used to visualize the mitochondria and a major mitochondrial component, cytochrome-c. An overlay photograph of saline control cells (Fig. 2A) displays a gold-colored, tubular network of intact, fused mitochondria, produced by the overlay of red (mitotracker) and green (cytochrome-c localized to mitochondria) fluorescence signal. In contrast, the cells pretreated with saline for 10 minutes and then exposed to H_2O_2 (100 μM) for 3 hours contain fragmented, punctate, red mitochondria with the green cytochrome-c dispersed throughout the cytosol (Fig. 2B). When the cells were preincubated with 10 nM HNG for 10 minutes prior to addition of the H_2O_2despite some punctate mitochondria and free cytochrome-c, much of the intact mitochondrial network was observed (Fig. 2C).

3.5. HNG increases cellular antioxidant activities

Levels of reduced glutathione (GSH) and the oxidized form (GSSG) were determined at various time points in the presence of either the control or HNG. The ratio of oxidized to reduced glutathione, a measure of oxidative stress, was decreased by 47% within 30 minutes of HNG treatment (0.2130 ± 0.0114 vs. 0.1131 ± 0.0179) (Fig. 3A).

The reduced form of glutathione is required to activate the critical antioxidant enzyme, glutathione peroxidase (GPx). This enzyme activity showed a 635% increase relative to control within the first 5 minutes of HNG treatment (98.26 ± 12.69 vs. 722.04 ± 253.09 mU/mg protein) (Fig. 3B). The activation decreased but remained significant throughout the 120 minutes investigated. Catalase, the other major antioxidant enzyme responsible for the removal of H_2O_2 was also activated within 5 minutes of HNG addition, producing a 213% increase in activity relative to controls (5.04 ± 0.46 vs. 15.78 ± 3.22 mU/mg protein) and was maintained at 30 minutes (Fig. 3C). Assay of total superoxide dismutase (SOD) activity demonstrated a 71% HNG-mediated enzyme activation by 120 minutes of treatment (1.63 ± 0.1483 vs. 2.78 ± 0.458 U/mg protein) (Fig. 3D).

3.6. A double knockdown of both Abl and Arg, but neither knocked down alone, eliminated the HNG-mediated reduction in oxidative stress

A pair of non-receptor tyrosine kinases, c-Abl and Arg have been demonstrated to participate in the post-translational activation of both catalase and GPx [20, 21]. We carried out transient, siRNA, Abl and Arg knockdowns in H_9C_2 cells and then assessed the ability of HNG to maintain the low intracellular ROS levels observed in HNG-treated WT cells. Results from siRNA knockdowns of c-Abl and Arg were verified at 72h post-transfection with qRT-PCR (Figure 4A). siRNA knockdown of Abl alone produced an 78% decrease in Abl mRNA (0.998 ± 0.001 vs. 0.218 ± 0.046). A double transfection with siRNAs for both Abl and Arg resulted in an 81% reduction in the Abl mRNA level (0.998 ± 0.001 vs. 0.191± 0.046). Arg knockdown produced a 79% loss of Arg mRNA relative to negative control knockdowns (0.998 ± 0.001 vs. 0.210 ± 0.024). The double knockdown decreased the Arg message level by 76% (.998 ± 0.001 vs. 0.242 ± 0.025). Immunoblots (Fig. 4B) provide evidence that the Abl and Arg knockdowns were also successful at the level of protein expression. We observed that negative control knockdown cells reiterate the data seen in Fig. 1A with WT cells, with H_2O_2 producing an increase in relative ROS in cells treated with the vehicle control (1.223 ± 0.335 vs. 2.347 ± 0.246). This increase was prevented by co-treatment with 10 nM HNG, with the DCF fluorescence value unchanged relative to the control and 94% lower than the control + H_2O_2 value (1.209 ± 0.254). This pattern was also observed following knockdown of either Abl or Arg, as loss of either of the kinases alone had no effect on the ability of HNG to maintain a low, control intracellular ROS level after addition of 100 μM H_2O_2 to the media. When Abl knockdowns were treated with H_2O_2HNG produced a 35% decrease in ROS relative to saline (2.442 ± 0.240 vs. 1.582 ± 0.241, for saline vs. HNG). For Arg knockdowns exposed to H_2O_2HNG lowered the cellular

ROS by 60% when compared to the effect of saline (2.252 ± 0.300 vs. 0.901 ± 0.339, for saline vs. HNG). In contrast, the cells with both Abl and Arg mRNA levels knocked down were no longer protected from oxidative stress by treatment with HNG and the relative ROS resulting from the H_2O_2 challenge matched that seen in the vehicle control (1.662 ± 0.366 vs 1.635 ± 0.325, for saline vs. HNG).

DISCUSSION

These findings demonstrate that HNG mitigates oxidative stress in a rat myoblast cell-line through rapid and sustained activation of several antioxidant enzymes that require the activity of one of a pair of non-receptor tyrosine kinases. The attenuation of oxidative stress results in preservation of mitochondrial membrane integrity and function.

Our findings are of significant clinical relevance as cardiac risk factors and resulting diseases that contribute to significant mortality and morbidity such as MI, cardiac failure, diabetes, atherosclerosis are all associated with ROS-induced cardiac damage. Free radical oxidants are also believed to contribute to the production of mitochondrial dysfunction and damage produced by the normal aging process [22]. Tissues such as cardiac muscle, with a high energy expenditure and abundant mitochondria, are particularly subject to mitochondrial oxidative damage, additional generation of ROS and further damage to critical molecular structures. ROS also stimulate the production of inflammatory cytokines from cardiac fibroblasts favoring a rise in collagen deposition and impaired cardiac function [23]. The ability of HNG to decrease cellular ROS and maintain mitochondrial integrity/function despite oxidative stress could explain the enhanced myocyte survival and the maintenance of cardiac function observed *in vivo* in MI-R models [18].

Both non-enzymatic and enzymatic antioxidant mechanisms appear to contribute to the observed oxidative stress reduction by HNG. The ratio of oxidized to reduced glutathione, a measure of oxidative stress, decreases within 30 minutes and the additional stores of reduced glutathione allows GPx to continue removing H_2O_2 from cells for the two hours observed in this study. Since catalase accounts for almost 80% of cardiomyocyte peroxidase activity [24], activation of both catalase and GPx within 5 minutes of HNG treatment and their sustained increases in activity can account for the rapid and persistent protection of the heart when HNG is provided just prior to reperfusion in the *in vivo* model of ischemia-reperfusion. The observed activation by HNG of total SOD in cardiac myoblasts supports recent similar observations in cortical neurons [25].

Since the rapid activation of catalase and GPx by HNG precludes *de novo* synthesis of these large enzymes, we focused on mechanisms that would produce their rapid, allosteric activation. The mammalian non-receptor, tyrosine kinase isoforms, Abl and Arg are constitutively repressed in the cytosol, requiring displacement of N-terminal and Src-homology regions from their kinase regions [26]. This displacement may be produced with physical interference from many different stimuli, allowing the enzyme to activate itself via autophosphorylation. Our results are consistent with the observations by Cao et al [20, 21] and show that either one of these isoforms is sufficient to retain the biologic effects of HNG in mitigating oxidative stress. Cells with an Abl knockdown but WT Arg levels could still use HNG to prevent an increase in ROS upon addition of H_2O_2. Despite a higher target protein expression in the Arg knockdowns, the phenotypic pattern seen in the Abl knockdowns was repeated. Both single knockdowns demonstrated a generalized increase in intracellular ROS levels at baseline relative to the negative knockdowns, while retaining the same pattern of protection from an additional oxidative challenge in the presence of HNG. In the presence of simultaneous knockdown of Abl and only a partial loss of Arg protein expression, HNG could no longer prevent the rise in intracellular ROS upon challenge with

H_2O_2. These studies provide evidence that HNG prevents oxidative stress via a mechanism requiring a critical level of activity from either Abl or Arg. The question of whether HNG itself physically interferes with the inactive conformations of Abl and Arg or whether it activates another required kinase suggests future areas of investigation.

Therapies that mitigate oxidative stress prevent the onset or progression of cardiac dysfunction through decreased apoptosis and increased cardiomyocyte survival. However, antioxidants alone have not proven to be clinically effective. Through its unique roles in substrate metaboilsm, decreased apoptosis and decreased ROS, HNG may offer translational promise as a cardioprotective factor in the clinical setting.

Acknowledgments

We thank Poojitha Kakulavaram and Sarah Silvestri for their technical assistance with the JC-10 assays.

Abbreviations

HN	Humanin, an endogenous 24-amino acid peptide
HNG	HN in which the serine 14 is replaced by glycine
MI-R	myocardial ischemia-reperfusion
ROS	reactive oxygen species
GPx	glutathione peroxidase
SOD	superoxide dismutase
MMP	mitochondrial membrane potential
c-Abl	Abelson murine leukemia viral mammalian homolog
Arg	Abl-related gene product

REFERENCES

1. Lloyd-Jones D, Adams R, Carnethon M, De Simone G, Ferguson TB, Flegal K, Ford E, Furie K, Go A, Greenlund K, Haase N, Hailpern S, Ho M, Howard V, Kissela B, Kittner S, Lackland D, Lisabeth L, Marelli A, McDermott M, Meigs J, Mozaffarian D, Nichol G, O'Donnell C, Roger V, Rosamond W, Sacco R, Sorlie P, Stafford R, Steinberger J, Thom T, Wasserthiel-Smoller S, Wong N, Wylie-Rosett J, Hong Y. Heart disease and stroke statistics--2009 update: a report from the American Heart Association Statistics Committee and Stroke Statistics Subcommittee. Circulation. 2009; 119:480–486. [PubMed: 19171871]
2. Giordano FJ. Oxygen, oxidative stress, hypoxia, and heart failure. J Clin Invest. 2005; 115:500–508. [PubMed: 15765131]
3. Pfeffer MA, Braunwald E. Ventricular remodeling after myocardial infarction. Experimental observations and clinical implications. Circulation. 1990; 81:1161–1172. [PubMed: 2138525]
4. Kevin LG, Camara AK, Riess ML, Novalija E, Stowe DF. Ischemic preconditioning alters real-time measure of O2 radicals in intact hearts with ischemia and reperfusion. Am J Physiol Heart Circ Physiol. 2003; 284:H566–H574. [PubMed: 12414448]
5. Ambrosio G, Zweier JL, Duilio C, Kuppusamy P, Santoro G, Elia PP, Tritto I, Cirillo P, Condorelli M, Chiariello M, et al. Evidence that mitochondrial respiration is a source of potentially toxic oxygen free radicals in intact rabbit hearts subjected to ischemia and reflow. J Biol Chem. 1993; 268:18532–18541. [PubMed: 8395507]
6. Venditti P, Masullo P, Di Meo S. Effects of myocardial ischemia and reperfusion on mitochondrial function and susceptibility to oxidative stress. Cell Mol Life Sci. 2001; 58:1528–1537. [PubMed: 11693531]

7. Lu FH, Tian Z, Zhang WH, Zhao YJ, Li HL, Ren H, Zheng HS, Liu C, Hu GX, Tian Y, Yang BF, Wang R, Xu CQ. Calcium-sensing receptors regulate cardiomyocyte Ca2+ signaling via the sarcoplasmic reticulum-mitochondrion interface during hypoxia/reoxygenation. J Biomed Sci. 2010; 17:50. [PubMed: 20565791]
8. Ong SB, Gustafsson AB. New Roles for Mitochondria in Cell Death in the Reperfused Myocardium. Cardiovasc Res. 2011
9. Ushio-Fukai M. Localizing NADPH oxidase-derived ROS. Sci STKE. 2006; 2006:re8. [PubMed: 16926363]
10. Veal EA, Day AM, Morgan BA. Hydrogen peroxide sensing and signaling. Mol Cell. 2007; 26:1–14. [PubMed: 17434122]
11. Hashimoto Y, Niikura T, Tajima H, Yasukawa T, Sudo H, Ito Y, Kita Y, Kawasumi M, Kouyama K, Doyu M, Sobue G, Koide T, Tsuji S, Lang J, Kurokawa K, Nishimoto I. A rescue factor abolishing neuronal cell death by a wide spectrum of familial Alzheimer's disease genes and Abeta. Proc Natl Acad Sci U S A. 2001; 98:6336–6341. [PubMed: 11371646]
12. Hoang PT, Park P, Cobb LJ, Paharkova-Vatchkova V, Hakimi M, Cohen P, Lee KW. The neurosurvival factor Humanin inhibits beta-cell apoptosis via signal transducer and activator of transcription 3 activation and delays and ameliorates diabetes in nonobese diabetic mice. Metabolism. 2010; 59:343–349. [PubMed: 19800083]
13. Sponne I, Fifre A, Koziel V, Kriem B, Oster T, Pillot T. Humanin rescues cortical neurons from prion-peptide-induced apoptosis. Mol Cell Neurosci. 2004; 25:95–102. [PubMed: 14962743]
14. Kariya S, Takahashi N, Hirano M, Ueno S. Humanin improves impaired metabolic activity and prolongs survival of serum-deprived human lymphocytes. Mol Cell Biochem. 2003; 254:83–89. [PubMed: 14674685]
15. Bachar AR, Scheffer L, Schroeder AS, Nakamura HK, Cobb LJ, Oh YK, Lerman LO, Pagano RE, Cohen P, Lerman A. Humanin is expressed in human vascular walls and has a cytoprotective effect against oxidized LDL-induced oxidative stress. Cardiovasc Res. 2010
16. Widmer RJ, Flammer A, Herrmann J, Rodriguez-Porcel M, Wan J, Cohen P, Lerman LO, Lerman A. Circulating humanin levels are associated with preserved coronary endothelial function. Am J Physiol Heart Circ Physiol. 2012
17. Zacharias DG, Kim SG, Massat AE, Bachar AR, Oh YK, Herrmann J, Rodriguez-Porcel M, Cohen P, Lerman LO, Lerman A. Humanin, a cytoprotective peptide, is expressed in carotid atherosclerotic [corrected] plaques in humans. PLoS One. 2012; 7:e31065. [PubMed: 22328926]
18. Muzumdar RH, Huffman DM, Calvert JW, Jha S, Weinberg Y, Cui L, Nemkal A, Atzmon G, Klein L, Gundewar S, Ji SY, Lavu M, Predmore BL, Lefer DJ. Acute humanin therapy attenuates myocardial ischemia and reperfusion injury in mice. Arterioscler Thromb Vasc Biol. 2010; 30:1940–1948. [PubMed: 20651283]
19. Lundin A, Hasenson M, Persson J, Pousette A. Estimation of biomass in growing cell lines by adenosine triphosphate assay. Methods Enzymol. 1986; 133:27–42. [PubMed: 3821540]
20. Cao C, Leng Y, Kufe D. Catalase activity is regulated by c-Abl and Arg in the oxidative stress response. J Biol Chem. 2003; 278:29667–29675. [PubMed: 12777400]
21. Cao C, Leng Y, Huang W, Liu X, Kufe D. Glutathione peroxidase 1 is regulated by the c-Abl and Arg tyrosine kinases. J Biol Chem. 2003; 278:39609–39614. [PubMed: 12893824]
22. Roede JR, Jones DP. Reactive species and mitochondrial dysfunction: mechanistic significance of 4-hydroxynonenal. Environ Mol Mutagen. 2010; 51:380–390. [PubMed: 20544880]
23. Souders CA, Bowers SL, Baudino TA. Cardiac fibroblast: the renaissance cell. Circ Res. 2009; 105:1164–1176. [PubMed: 19959782]
24. Pendergrass KD, Varghese ST, Maiellaro-Rafferty K, Brown ME, Taylor WR, Davis ME. Temporal effects of catalase overexpression on healing after myocardial infarction. Circ Heart Fail. 2011; 4:98–106. [PubMed: 20971939]
25. Zhao ST, Huang XT, Zhang C, Ke Y. Humanin protects cortical neurons from ischemia and reperfusion injury by the increased activity of superoxide dismutase. Neurochem Res. 2012; 37:153–160. [PubMed: 21935731]
26. Woodring PJ, Hunter T, Wang JY. Regulation of F-actin-dependent processes by the Abl family of tyrosine kinases. J Cell Sci. 2003; 116:2613–2626. [PubMed: 12775773]

Highlights

- HNG prevents increased ROS levels in cardiac myoblasts exposed to H_2O_2.
- HNG protects mitochondrial membrane potential and function from H_2O_2.
- The ratio of oxidized to reduced glutathione is decreased in the presence of HNG.
- HNG treatment produces rapid and sustained activation of major antioxidant enzymes.
- Abl or Arg is required for HNG to maintain ROS levels in the presence of H_2O_2.

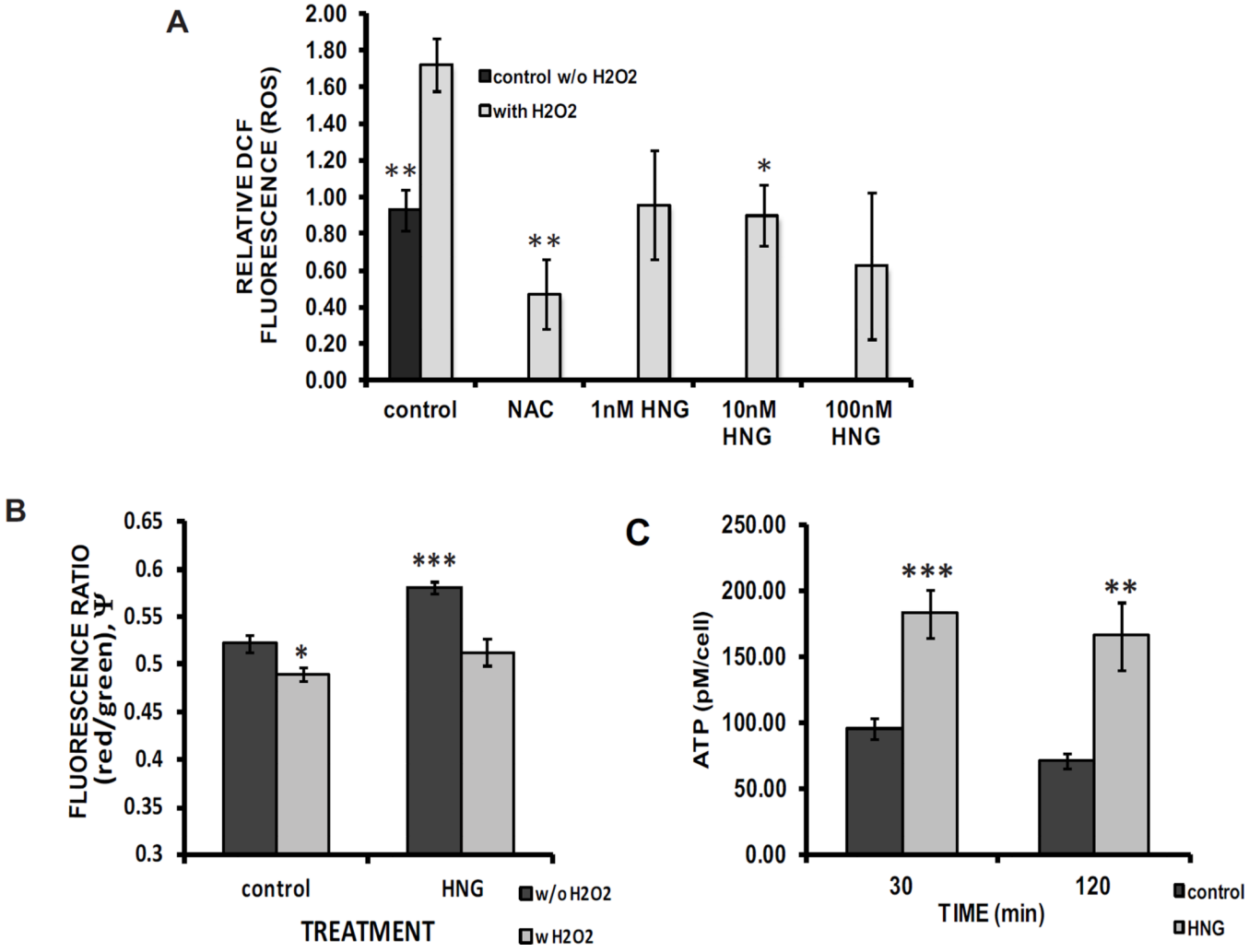

Fig. 1. HNG prevents oxidative stress, maintains inner mitochondrial membrane potential (Δψm) and mitochondrial function

A Relative DCF fluorescence in saline controls, controls exposed to 100 μM $H_2O_2$and cells incubated in HNG (10 nM) with 100 μM H_2O_2 (* compared with H_2O_2-treated control, p = 0.003, ** p =0.001; 8 N per experiment, 7 experiments). B The ratio of red/green fluorescence (ψm) from JC-10 loaded cells that had been pretreated with 40 μM H_2O_2 with or without HNG (10 nM) (compared with control treated cells, no H_2O_2*p = 0.0142, *** p = 5.0×10^{-6}15 N per experiment, 3 experiments). C Intracellular ATP levels after 30 and 120 minutes of HNG exposure (compared with matched control, ** p = 0.0024, *** p = 0.0001, 3 N per experiment, 4 experiments).

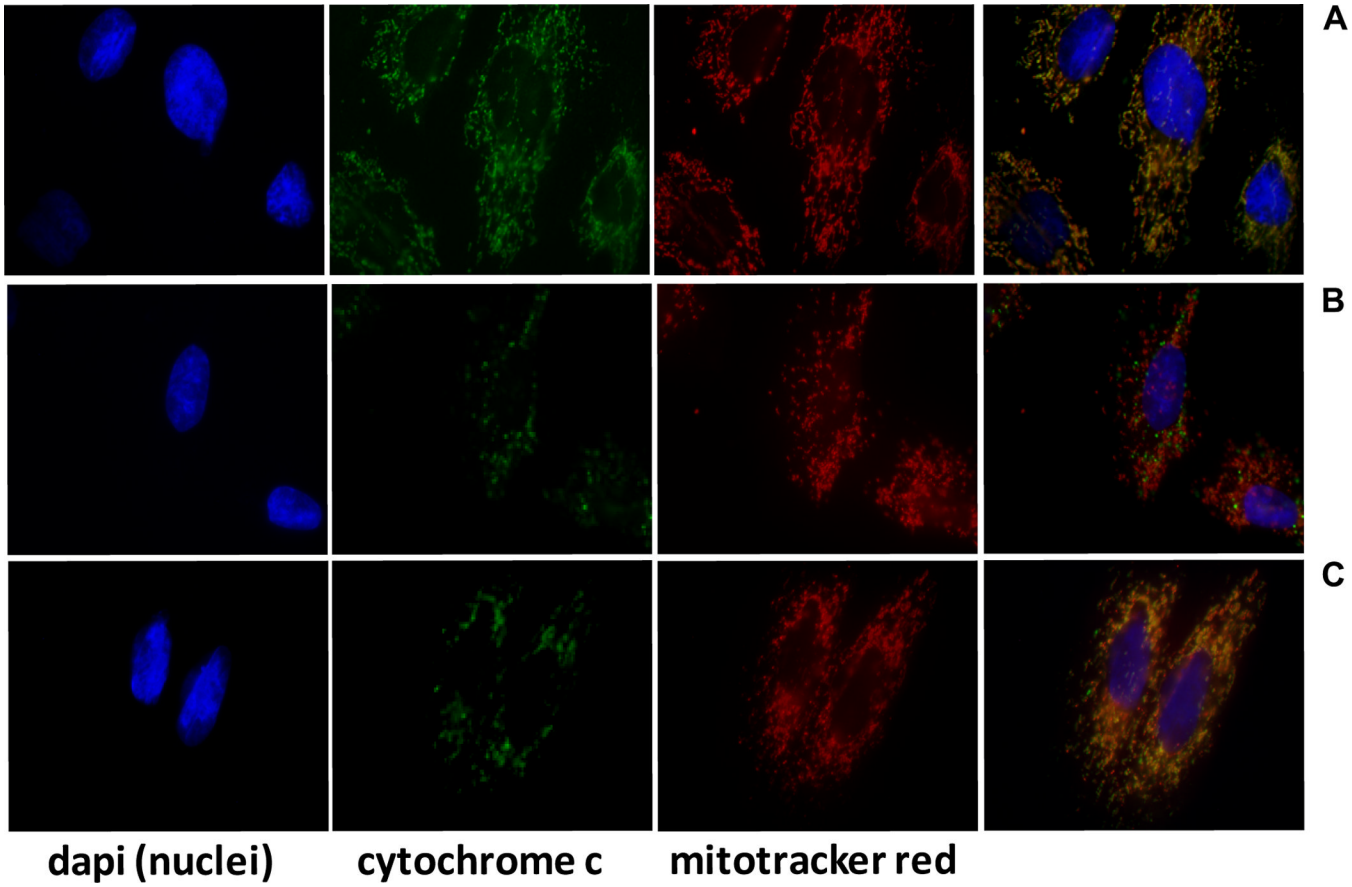

Fig. 2. Immunofluorescent overlays support HNG-mediated preservation of mitochondrial structure

A saline controls, B saline for 10 minutes followed by addition of H_2O_2 (100 μM, 3 hours), C HNG (10 nM) for 10 minutes, then as in B. blue: Dapi stained nuclei, green: cytochrome c, red: MitotrackerCMXROS, 63× magnification.

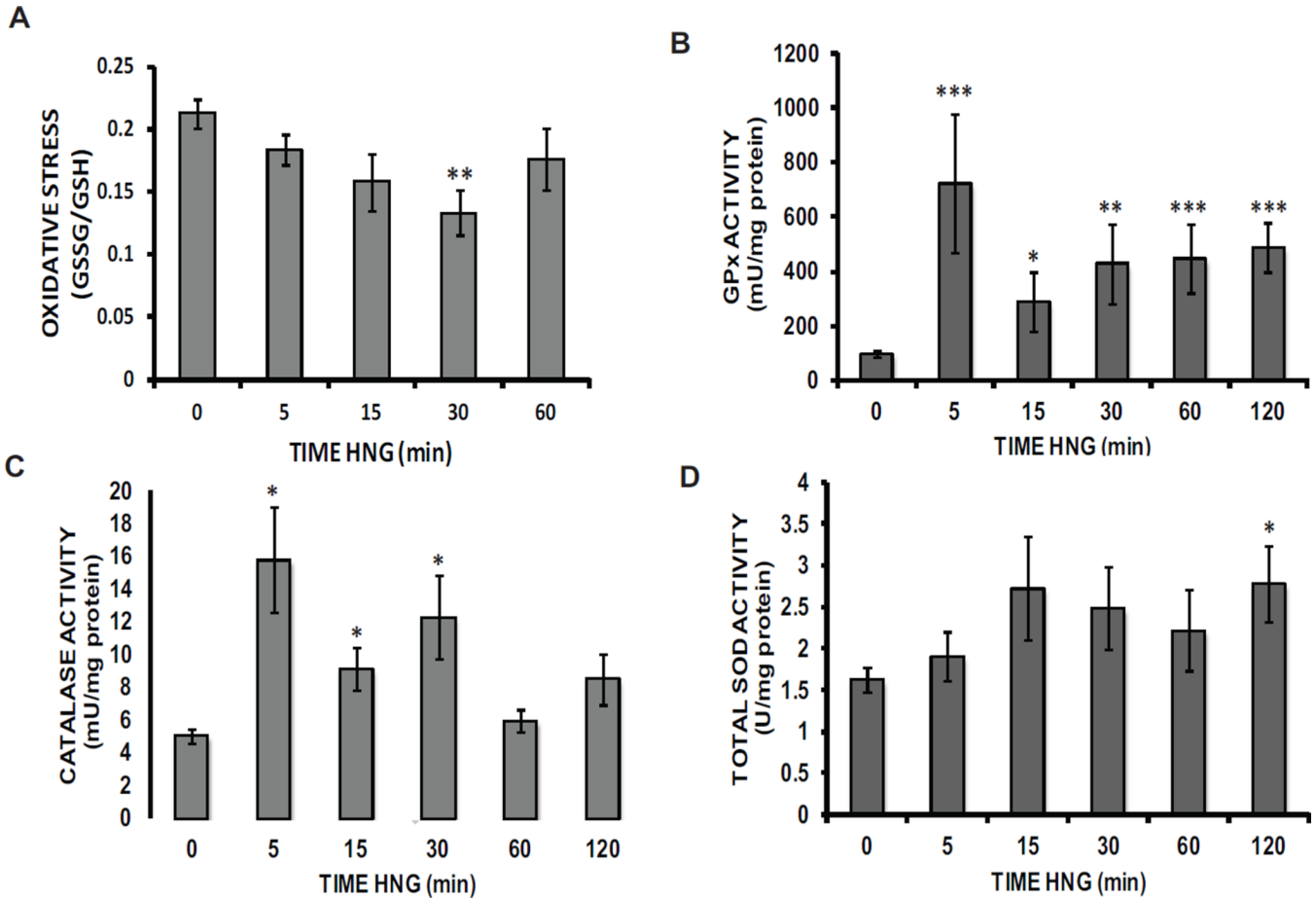

Fig. 3. HNG decreases a glutathione-based measure of oxidative stress while rapidly and persistently enhancing the activity of critical antioxidant enzymes

A The time course of change in the ratio of oxidized to reduced glutathione in lysates of cells treated with HNG (10 nM) (***p* = 0.0007, 10 N per experiment, 4 experiments). Both **B** GPx (***p* = 4.0×10^{-6}7 N per experiment, 4 experiments) and **C** catalase (**p* = 0.0089, 18 N per experiment, 6 experiments) activities, normalized to total protein, following cell exposure to HNG (10 nM) and lysate prep. **D** Total cellular SOD activity (normalized to total protein) in lysates from cells exposed to HNG (10 nM) (**p* = 0.004, 12 N per experiment, 4 experiments).

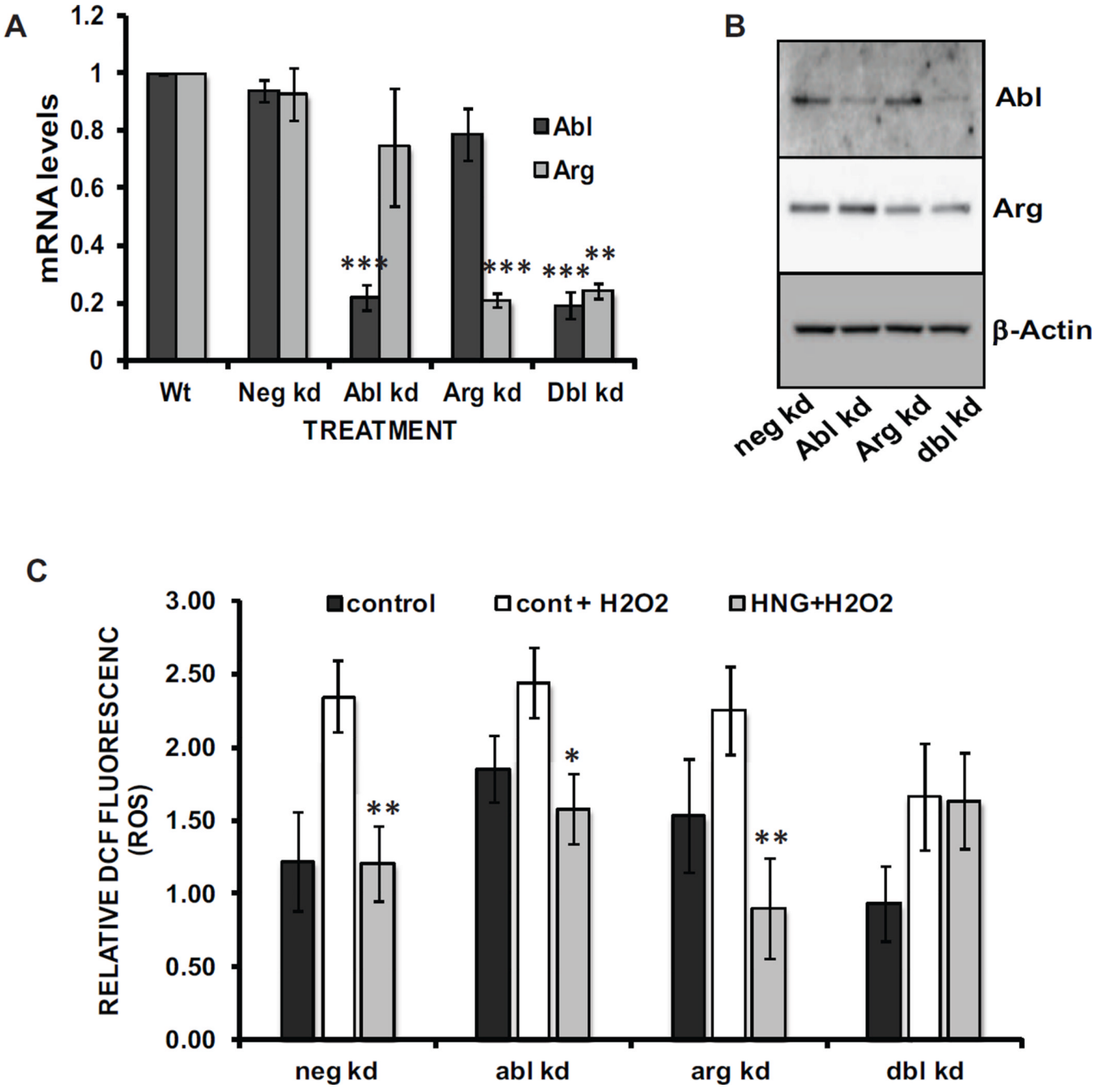

Fig. 4. Abl and Arg mRNA knockdowns demonstrate that one must be functional for HNG-mediated ROS reduction

A qRT-PCR results for siRNA knockdowns of Abl and Arg, each alone and in combination with the other (*** $p = 0.0009$, n=3). B Immunoblots prepared with lysates from cells treated as in A. C Following siRNA transfections, relative intercellular ROS levels were determined as described for Figure 1. (*$p = 0.0139$, **$p = 0.003$ for neg kd, and 0.005 for arg kd, 18 N per experiment, 3 experiments).